Investigation on the Interaction of Newly Designed Anticancer Pd(II) Complexes with Different Aliphatic Tails and Human Serum Albumin

Adeleh Divsalar,*,†,‡ Mohammad Javad Bagheri,† Ali Akbar Saboury,† Hassan Mansoori-Torshizi,§ and Mojtaba Amani||

Institute of Biochemistry and Biophysics, University of Tehran, Tehran, Iran, Department of Biological Sciences, Tarbiat Moallem University, Tehran, Iran, Department of Chemistry, University of Sistan & Baluchestan, Zahedan, Iran, and Department of Biochemistry, Ardabil University of Medical Sciences, Ardabil, Iran

Received: May 23, 2009; Revised Manuscript Received: July 27, 2009

The pharmacokinetics and pharmacodynamics of any drug will depend, largely, on the interaction that it has with human serum albumin (HSA), the most abundant plasma protein. The interaction between newly synthesized Pd(II) complexes, 2,2′-bipyridin octyl dithiocarbamato Pd(II) nitrate (Octpd), 2,2′-bipyridin butyl dithiocarbamato Pd(II) nitrate (ButPd), 2,2′-bipyridin ethyl dithiocarbamato Pd(II) nitrate (EtPd), antitumor components, with human serum albumin, a carrier protein, were studied at different temperatures of 27 and 37 °C by fluorescence spectroscopy, far UV circular dichroism (CD), and spectrophotometric and differential scanning calorimetry (DSC) techniques. By the analysis of fluorescence intensity, it was observed that Pd(II) complexes have strong abilities to quench the intrinsic fluorescence of HSA through a dynamic quenching procedure. The binding parameters were evaluated by the fluorescence quenching method. The thermodynamic parameters, including $\Delta H°$, $\Delta S°$, and $\Delta G°$, were calculated by the fluorescence quenching method and indicated that hydrophobic forces play a major role in the interaction of Pd(II) complexes with HSA. Far-UV-CD results represented that Pd(II) complexes induced a decrease in content of the α helical structure of protein. The binding of newly designed drugs (Pd(II) complexes) on the blood carrier protein of HSA resulted in significant alterations on the structure and conformation of protein via decreasing stability of HSA by decreasing the T_m, a red shift in maximum fluorescence intensity, a decrease in content of the α-helical structure, and the increase of the nonpolar or accessible hydrophobic surface of HSA to solvent.

Introduction

Human serum albumin (HSA) is the most abundant protein constituent of blood plasma and serves as a protein storage component. Its three-dimensional structure has been determined through X-ray crystallographic measurements. This protein is a single-chain 66 kDa protein, which is largely α-helical and consists of three structurally homologous domains that assemble to form a heart-shaped molecule.[1,2] Each domain is a product of two subdomains, which are predominantly helical and extensively cross-linked by several disulfide bridges. Its amino acid sequence contains a total of 17 disulfide bridges, one free thiol (Cys 34), and a single tryptophan (Trp-214).[3,4]

HSA can bind and carry through the bloodstream many drugs, which are poorly soluble in water.[5,6] It has been shown that the distribution, free concentration, and metabolism of various drugs can be significantly altered as a result of their binding to HSA.[7] Drug interactions at the protein binding level will in most cases significantly affect the apparent distribution volume of the drugs and also affect the elimination rate of drugs; therefore, the studies on this aspect can provide information on the structural features that determine the therapeutic affectivity of drugs and have been an interesting research field in life sciences, chemistry, and clinical medicine.[8−10]

The discovery of *cis*-platinum compounds as an antitumor drug has prompted intensive research into the development of compounds with lower toxicity and higher selectivity toward the tumor cells.[11] Platinum(II) complexes including *cis*-platin and carboplatin are widely used in the treatment of several human malignant diseases, such as ovarian, testicular, lung, urinary bladder, head, and neck cancer.[12,13] However, *cis*-platin and its analogues produce several side effects including nephrotoxicity, coming out in injury to renal tubular epithelial cells and can be revealed as either acute renal failure or a chronic syndrome characterized by renal electrolyte wasting.[12,14] Several reports have demonstrated that the binding of platinum complexes to the N7-nitrogens of two adjacent guanosine bases is thought to disrupt DNA duplication leading to cell death. However, platinum complexes are also known to react with many other cell components including glutathione and other S-containing biomolecules, present in relatively high doses inside the cell.[15,16] Recent studies have shown that platinum complexes can bind and inactivate the thiol-containing enzymes of the renal and have serious side effects on the kidney.[12,16] Because palladium chemistry is similar to that of platinum, it was speculated that Pd complexes might also exhibit antitumor activities with lower side effects than platinum(II) complexes. Attempts have been made to synthesize Pd(II) complexes with such activities. Palladium complexes are expected to have lower kidney toxicity than *cis*-platin due to their inability to replace the tightly bound chelate ligands of Pd(II) with sulfhydryl groups of protein kidney tubules.[14,17,15] Our group[18] and others[16,19,20] have reported that Pd(II) complexes also have significant

* To whom correspondence should be addressed. E-mail: divsalar@ibb.ut.ac.ir. Phone: 0098 21 61113381. Fax: 0098 21 66404680.
† University of Tehran.
‡ Tarbiat Moallem University.
§ University of Sistan & Baluchestan.
|| Ardabil University of Medical Sciences.

10.1021/jp904822n CCC: $40.75
Published on Web 09/24/2009

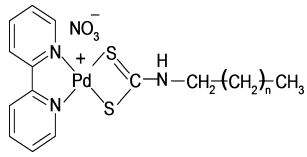

Figure 1. Molecular structure of complexes: $n = 6$, OctPd(II) complex; $n = 2$, ButPd(II) complex; and $n = 0$, EtPd(II) complex.

cytotoxicity against some human tumor cell lines. Genova et al.[19] have shown that Pd(II) complexes exhibit a significant activity against acyclovir-resistant viruses R-100 (HSV 1) and PU (HSV 2) and also negatively influenced the expression of key structural HSV-1 proteins (VP 23, gH, and gG/gD), thus suppressing simultaneously virus entry, transactivation of virus genome, capsid assembly, and cell-to-cell spread of infectious HSV progeny.[19]

Since several reports have represented that Pd(II) complexes containing dithiol group have low side effects especially on the kidney, we decided to investigate the effects of three new Pd(II) complexes (Figure 1) with different hydrophobic tails on the structure of the blood carrier protein of HSA and represented the effects of different temperatures (27 (room temperature) and 37 °C (physiologic temperature)) on the transport ability and type of interactions for HSA under interaction with these Pd(II) complexes.

Experimental Section

Materials. Human serum albumin (HSA) was purchased from Sigma. 2,2′-Bipyridin ethyl dithiocarbamato Pd(II) nitrate, 2,2′-bipyridin butyl dithiocarbamato Pd(II) nitrate, and 2,2′-bipyridin octyl dithiocarbamato Pd(II) nitrate (Figure 1) were synthesized in our laboratory using previous procedures.[12,21] All other materials and reagents were of analytical grade, and solutions were made in double-distilled water. NaCl solution, with 5 mM concentration, was used as a solvent. Since Pd(II) complexes did not dissolve in any buffers with pH 7, then we have to dissolve them in NaCl (5 mM). Concentrations of HSA were determined spctrophotometrically by using, for the calculation, a molecular absorption coefficient of $\varepsilon^{10}{}_{278\ nm} = 5.3\ M^{-1}\ cm^{-1}$.

Methods. ***Fluorescence Measurements.*** Fluorescence intensity measurements were carried out on a Cary spectrofluorimeter model. The excitation wavelength was adjusted at 280 nm, and the emission spectra were recorded for all of the samples at different temperatures (27 and 37 °C) in the range of 300−500 nm. Measurements were made by applying a 1 cm path length fluorescence cuvette and slit width of 5 nm. The fluorescence intensities of the Pd(II) complexes at the highest denaturant concentration at excitation 280 nm have been checked, and the magnitudes of the emissions of these compounds were very small and negligible. The concentration of the protein (HSA) in fluorescence studies was 4.5 μM.

The binding of a hydrophobic fluorescent probe, ANS, to HSA was monitored by exciting the ANS (135 μM) at 350 nm and recording the emission spectra in the range of 400−600 nm. All measurements were made using a 1 cm path length fluorescence cuvette. The extrinsic fluorescence spectra of the HSA (4.5 μM) were measured in the absence and presence of 22, 44, and 65.7 μM of the Pd(II) complex at different temperatures of 27 and 37 °C.

CD Measurements. CD spectra were recorded on an Aviv Spectropolarimeter model 215. Changes in the secondary structures of HSA were monitored in the far UV region (200−260 nm) using 0.1 cm path length cells, with a resolution of 0.2 nm, scan speed of 20 nm min^{-1}, time constant of 2.0 s, 10 nm bandwidth, and sensitivity of 20 A°. The protein concentration in the experiments for the far UV region was 3.7 μM. Alterations in the secondary structure of the protein were investigated in the absence and presence of different concentrations of Pd(II) complexes (0, 41, 82, and 123 μM). The results were expressed in molar ellipticity $[\theta]$ (deg cm^2 $dmol^{-1}$) based on a mean amino acid residue weight of 113.7 (MRW). The molar ellipticity was determined as $[\theta]_\lambda = (100 \times MRW \times \theta_{obs}/cl)$, where θ_{obs} is the observed ellipticity in degrees at a given wavelength; c is the protein concentration in milligrams per milliliter; and l is the length of the light path in millimeters. The CD software was used to predict the secondary structure of the protein according to the statistical method.[22,23]

Differential Scanning Calorimetry Measurements. Thermal denaturation of HSA in the absence and presence of different Pd(II) complexes was studied by differential scanning calorimetry (DSC) using a Scal 1 differential scanning microcalorimeter equipped with 0.355 mL capillary glass cells, under 2 atm of pressure over cells. The temperature range of 10−90 °C was scanned with a scan rate of 0.5 °C/min. Protein concentration was 1 mg/mL. The calorimetric data were analyzed by the Scan Scal C program, and the excess C_p (in kJ K^{-1} mol^{-1}) was finally plotted as a function of temperature. The T_m of the denaturation process was calculated as the temperature with the maximal excess C_p.

Results and Discussion

The binding of a ligand to a protein may directly affect the fluorescence of a tryptophan residue by acting as a quencher or by physically interacting with the fluorophore, thereby changing the polarity of its environment and/or its accessibility to solvent. Both direct and generalized effects may result in either the enhancement or quenching of fluorescence and/or red or blue spectrum shifts. Quenching can occur by different mechanisms, which are usually classified as dynamic quenching and static quenching. Dynamic and static quenching can be distinguished by their differing dependence on temperature and viscosity. Dynamic quenching depends upon diffusion. Since higher temperatures result in larger diffusion coefficients, the bimolecular quenching constants are expected to increase with increasing temperature. In contrast, increased temperature is likely to result in decreased stability of complexes of protein−ligand and thus lower values of the static quenching constants.[24−27]

There is one tryptophan residue in HSA, Trp214, which is situated in hydrophobic subdomain IIA, one of the two principal binding sites on HSA.[28] Figure 2(A−C) shows the intrinsic fluorescence of the HSA in the presence of different complexes of EtPd, ButPd, and OctPd at 27 °C. As shown in Figure 2(A−C), the Pd(II) complexes reduce the intrinsic fluorescence emission of HSA markedly at different concentrations and then quench it, and red shifts (approximately 13−20 nm) are observed in a maximum emission wavelength (λ_{max}), which is probably owing to the loss of the compact structure of the hydrophobic region where the Trp residue is placed. Insets of Figure 2(A−C) represent the intrinsic fluorescence of HSA at 335 nm at temperatures of 27 and 37 °C with varying concentrations of different Pd(II) complexes. A maximal quenching is reached at different concentrations of compounds depending on the type of complexes. As is shown in the insets of Figure 2(A−C), by increasing the aliphatic tail of complexes from ethyl up to octyl, the maximal quenching in the fluorescence intensity is observed in higher concentrations of Pd(II) complexes.

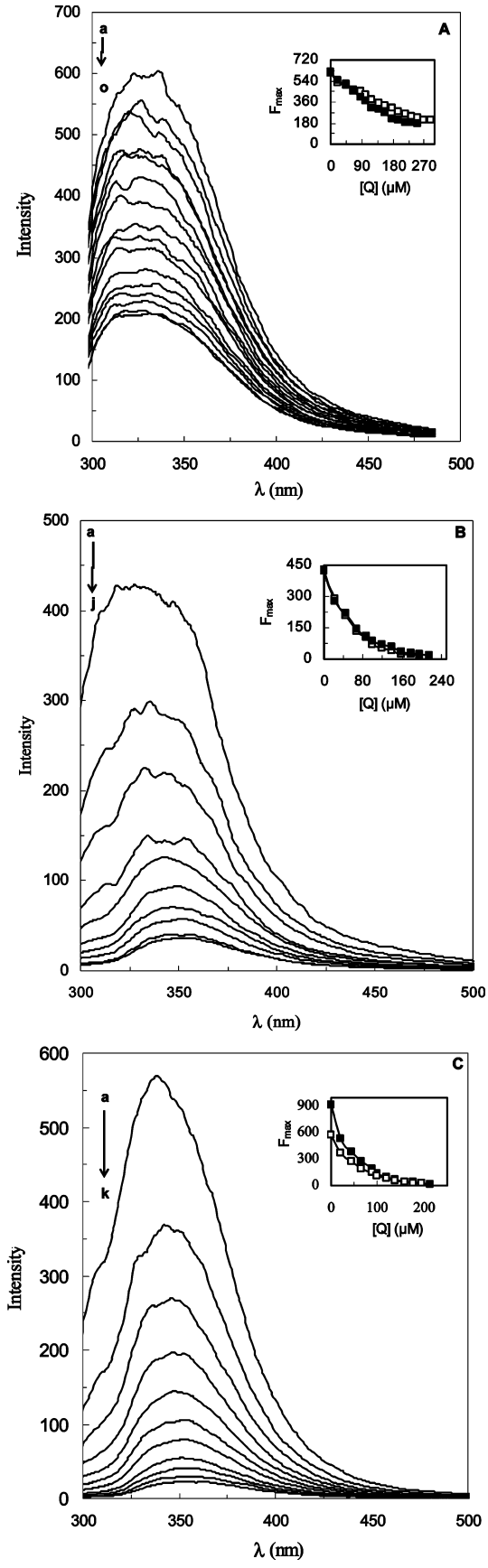

Figure 2. (A) Fluorescence titration curve of HSA (4.5 μM) with the OctPd(II) complex in 5 mM NaCl solution, pH 7.4, at 27 °C. (B) The fluorescence titration curve of HSA (4.5 μM) with the ButPd(II) complex in 5 mM NaCl solution, pH 7.4, at 27 °C. (C) The fluorescence titration curve of HSA (4.5 μM) with the EtPd(II) complex in 5 mM NaCl solution, pH 7.4, at 27 °C.

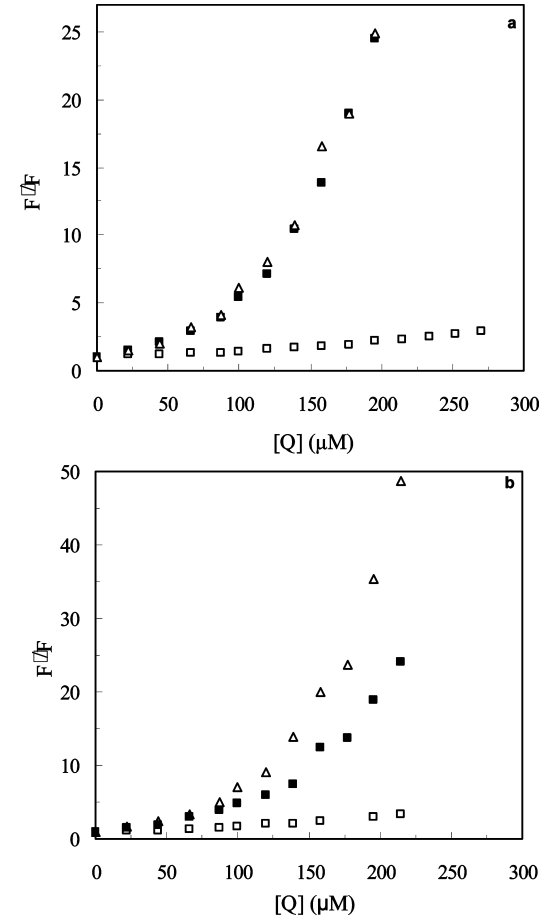

Figure 3. (a) Stern−Volmer plot for quenching of different Pd(II) complexes: octyl (□), butyl (■), and ethyl (Δ), to HSA in 5 mM NaCl solution at 27 °C. (b) Stern−Volmer plot for quenching of different Pd(II) complexes: octyl (□), butyl (■), and ethyl (Δ), to HSA in 5 mM NaCl solution at 37 °C.

Several reports have shown that the fluorescence intensity of a compound can be decreased by a variety of molecular interactions including excited-state reactions, molecular rearrangements, energy transfer, ground state complex formation, and collisional quenching. Such a decrease in intensity is called quenching.[29,30] The different mechanisms of quenching are usually classified as either dynamic quenching or static quenching. Dynamic and static quenching can be distinguished by their differing dependence on temperature and viscosity.[31] The role of fluorescence quenching can be studied experimentally by determining quenching rate parameters using Stern−Volmer plots.[32] The intrinsic fluorescence spectra of HSA was strongly quenched by addition of Pd(II) complexes at different temperatures. To speculate the fluorescence quenching mechanism, the fluorescence quenching data for HSA were first analyzed using the classical Stern−Volmer equation (eq 1)

$$\frac{F_0}{F} = 1 + K_{SV}[Q] \quad (1)$$

where F_0 and F are the fluorescence intensities of the HSA in the absence and presence of different Pd(II) complexes, respectively. K_{SV} is the Stern−Volmer dynamic quenching constant and [Q] is the total concentration of the quencher (in this case, Pd(II) complexes). The fluorescence quenching data of HSA in the presence of different complexes at two temper-

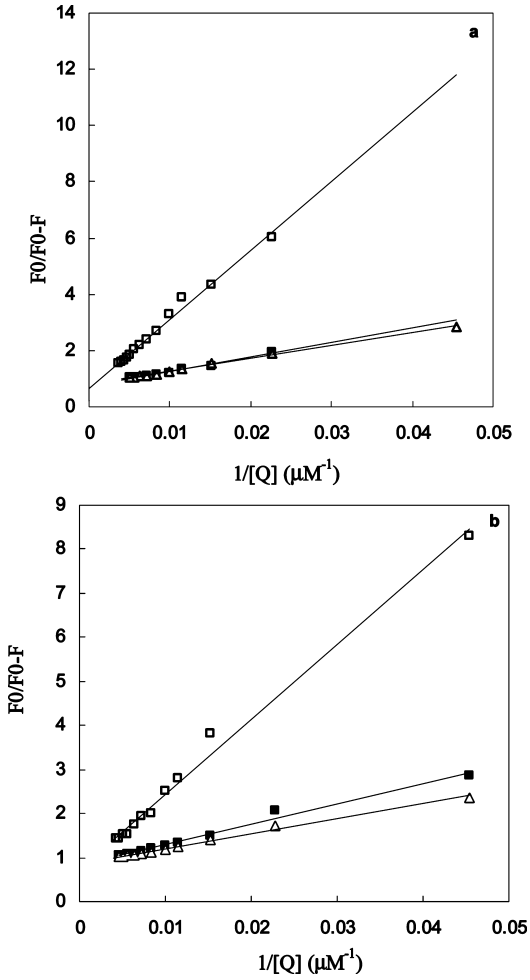

Figure 4. (a) Best linear plot of $F_0/F_0 - F$ versus 1/[Q] according to eq 2 at 27 °C: octyl (□), butyl (■), and ethyl (Δ). (b) The best linear plot of $F_0/F_0 - F$ versus 1/[Q] according to eq 2 at 37 °C: octyl (□), butyl (■), and ethyl (Δ).

TABLE 1: Various Parameters of HSA upon Interaction with Pd(II) Complexes at Two Temperatures of 27 and 37 °C

Pd(II) complexes at different temperatures (°C)		[a]n	[b]K (μM^{-1})	[c]K_{SV} (μM^{-1})	[d]$\Delta H°$ kJ/mol	[e]$\Delta G°$ kJ/mol	[f]$\Delta S°$ J/mol K	[g]f_a
Et	27	2.09	309	17.454	−3.7	−14.3	35.3	1.2
	37	2.18	278	25.266		−14.0	33.2	1.2
But	27	2.1	292	14.09	24.3	−14.1	128	1.4
	37	1.99	423	17.743		−15.1	127.1	1.2
Oct	27	1.2	122	2.437	41.7	−17.7	198	1.5
	37	1.2	210	4.299		−19.1	196	1.4

[a] Number of binding sites. [b] Apparent association constant,. [c] Values of Stern−Volmer constants,. [d] Values of the enthalpy ($\Delta H°$). [e] Values of the Gibbs free energy ($\Delta G°$). [f] Values of entropy of binding ($\Delta S°$). [g] The fraction of fluorescence accessible to quenching (f_a).

atures of 27 and 37 °C, matched by eq 1, are shown in Figure 3a and 3b, respectively. The plots of F_0/F versus [Q] showed positive deviation (Figure 3a and b). From these results, it can be concluded that Pd(II) complexes bound to HSA and the HSA−Pd complexes formed, resulting in a fluorescence quenching of the fluorophore. These results indicate that the probable quenching mechanism of Pd(II)−HSA binding reactions are initiated by compound formation rather than by dynamic collision.

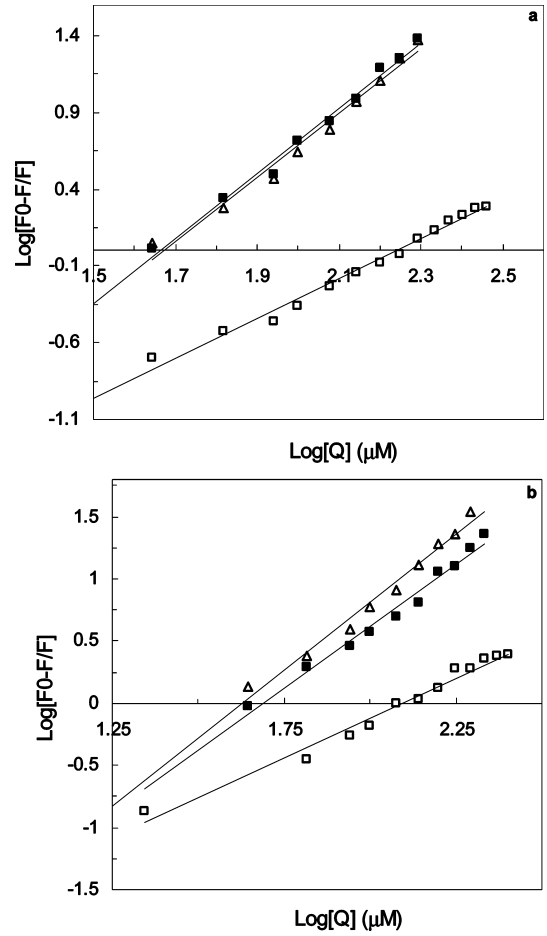

Figure 5. (a) Best linear plot of F_0/F versus [Q] × $(F_0/F_0 - F)$ according to the eq 3. Values of K_A and n of binding of Pd(II) complexes (octyl (□), butyl (■), and ethyl (Δ)) to HSA can be obtained from the slope and the vertical intercepts, respectively, at 27 °C. (b) The best linear plot of F_0/F versus [Q] × $(F_0/F_0 - F)$ according to eq 3. Values of K_A and n of binding of Pd(II) complexes (octyl (□), butyl (■), and ethyl (Δ)) to HSA can be obtained from the slope and the vertical intercepts, respectively, at 37 °C.

Therefore, the quenching data were analyzed according to the modified Stern−Volmer equation[33,34]

$$\frac{F_0}{(F_0 - F)} = \frac{1}{f_a} + \frac{1}{f_a K_{SV}} \frac{1}{[Q]} \qquad (2)$$

where f_a is the fraction of the initial fluorescence, which is accessible to the quencher. The value of f_a refers to the fraction of fluorescence accessible to quenching, which need not be the same as the fraction of tryptophan residue accessible to quenching.[35] The dependence of $F_0/(F_0 - F)$ on the reciprocal value of the quencher concentration (1/[Q]) is linear. The values of f_a and K_{SV} were obtained from the values of intercept and slope, respectively (Figure 4a and b). The values of f_a for HSA in the presence of complexes of EtPd, ButPd, and OctPd(II) at two temperatures of 27 and 37 °C were found and indicate that 80, 73, and 67% at 27 °C and 86, 82, and 73% at 37 °C, respectively, of the total fluorescence of HSA were accessible to quenchers (different Pd(II) complexes), and the others, 20, 27, and 33% (at 27 °C, respectively) and 14, 18, and 27% (at 37 °C, respectively) are not affected by Pd(II) complexes (Figure 4a and b). These results significantly revealed that complexes with longer hydrophobic tails have lower ability to quenching

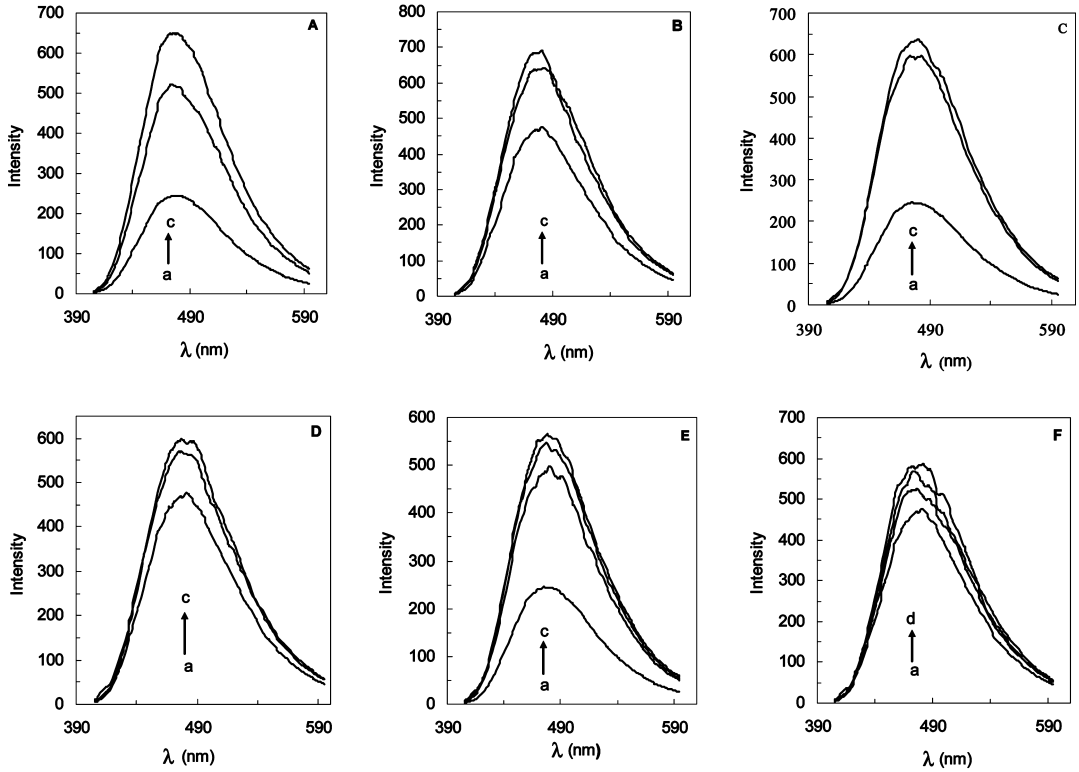

Figure 6. (A) ANS fluorescence curve of HSA (4.5 μM) with Pd(II) complexes of octyl in the presence of ANS at 27 °C. (B) The fluorescence titration curve of HSA (4.5 μM) with the Pd(II) complex of octyl in the presence of ANS at 37 °C. (C) The fluorescence titration curve of HSA (4.5 μM) with the Pd(II) complex of butyl in the presence of ANS at 27 °C. (D) The fluorescence titration curve of HSA (4.5 μM) with the Pd(II) complex of butyl in the presence of ANS at 37 °C. (E) The fluorescence titration curve of HSA (4.5 μM) with the Pd(II) complex of ethyl in the presence of ANS at 27 °C. (F) The fluorescence titration curve of HSA (4.5 μM) with the Pd(II) complex of ethyl in the presence of ANS, at 37 °C.

and accessibility to the Trp residue of protein. The Stern−Volmer quenching constant was calculated and listed in Table 1. As seen in Table 1, values of Stern−Volmer quenching constants (K_{SV}) are explicitly dependent on temperature. On the other hand, it can be seen that by increasing the temperatures from 27 to 37 °C the values of K_{SV} were increased indicating the highest contribution of dynamic mechanism of quenching.

Analysis of Binding Equilibria. Florescence quenching data from interaction of complexes and HSA were analyzed to obtain various binding parameters. The binding constant (K) and number of binding (n) were calculated according to the equation[36]

$$\log \frac{F_0 - F}{F_0} = \log K + n \log[\mathrm{Q}] \qquad (3)$$

where F_0 and F are the florescence intensity without and with the Pd(II) complexes, respectively. A plot of $\log[(F_0 - F)/F]$ vs $\log[\mathrm{Q}]$ gave a straight line using least-squares analysis whose slope was equal to n (binding site number) and the intercept on the Y-axis to $\log K$ (K = binding constant) (Figure 5a and b). The slope of the regression curve (n) of the complexes was calculated at two temperatures of 27 and 37 °C. The binding site numbers (n) for ethyl−, butyl−, and octyl−Pd(II) complexes are 2.1, 2.1, and 1.3 (at 27 °C, respectively) and 2.1, 2.0, and 1.3 (at 37 °C, respectively). It means that one molecule of octyl complex and two molecules of each butyl and ethyl complexes combine with one molecule of HSA at both 27 and 37 °C. The association constants calculated for the complexes−HSA suggest high affinity Pd(II) complexes−HSA binding, compared to the other strong ligand−protein complexes. However, lower binding constants (10^4 to 10^5 M^{-1}) were also reported for several other ligand−protein complexes using fluorescence spectroscopic methods.[36] Also, the binding constant for EtPd(II)−HSA is the highest.

Considering the dependence of binding constant on temperature, a thermodynamic process was considered to be responsible for the formation of the complex.[36,26] Therefore, the dependence of thermodynamic parameters on the temperature was analyzed to further characterize the acting forces between Pd(II) complexes and HSA. The acting forces between a small molecule and macromolecule include hydrogen bond, van der Waals force, electrostatic force, hydrophobic interaction force, and so on.[37,38] The thermodynamic binding parameters of enthalpy change ($\Delta H°$) were determined using the van't Hoff equation[38]

$$\frac{\ln K_2}{\ln K_1} = \frac{-\Delta H°}{R}\left(\frac{1}{T_2} - \frac{1}{T_1}\right) \qquad (4)$$

The above equation enables determination of $\Delta H°$ of the binding process. The values of Gibbs free energy change ($\Delta G°$) and entropy ($\Delta S°$) were calculated using eqs 5 and 6[38]

$$\Delta G° = -RT \ln K \qquad (5)$$

$$\Delta G° = \Delta H° - T\Delta S° \qquad (6)$$

where R is the gas constant. The values of $\Delta H°$, $\Delta S°$, and $\Delta G°$ have been summarized in Table 1. Results of Table 1 show

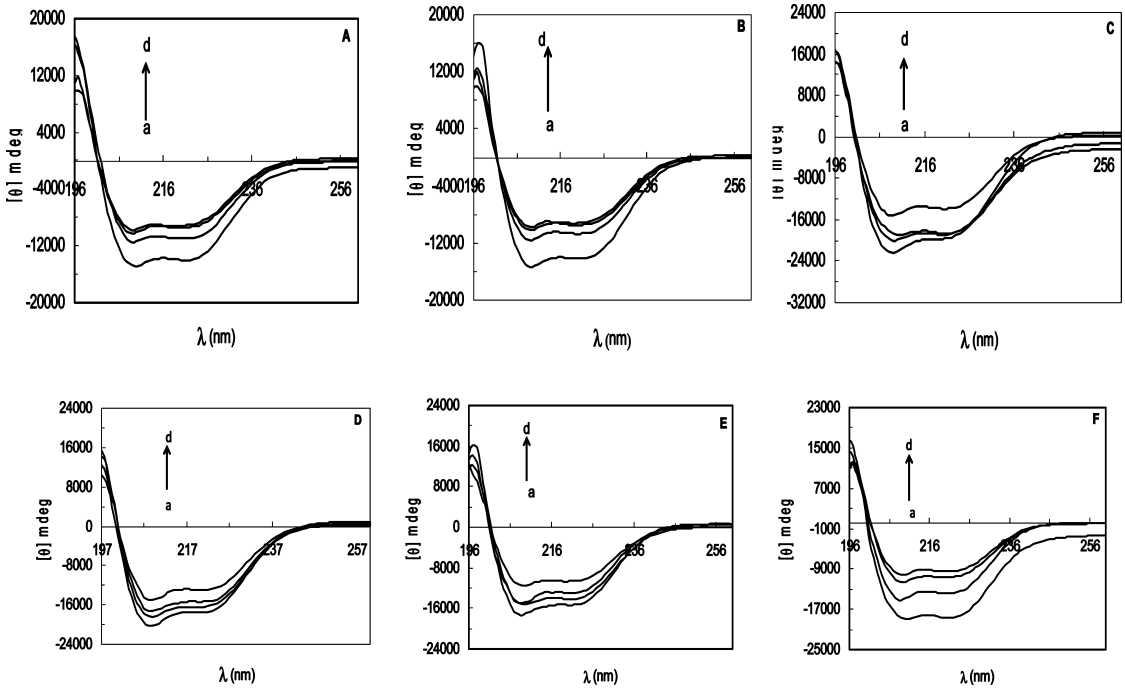

Figure 7. (A) Far-UV-circular dichorism spectra of 3.7 μM HSA measured in the absence (a) and presence of different concentrations of OctPd(II): 41.1 (b), 82.1(c), and 123.2 (d) μM at a temperature of 27 °C in 5 mM sodium chloride solution. (B) Far-UV-circular dichorism spectra of 3.7 μM HSA measured in the absence (a) and presence of different concentrations of OctPd(II): 41.1 (b), 82.1 (c), and 123.2 (d) μM at temperature 37 °C in 5 mM sodium chloride solution. (C) Far-UV-circular dichorism spectra of 3.7 μM HSA measured in the absence (a) and presence of different concentrations of ButPd(II): 41.1 (b), 82.1 (c), and 123.2 (d) μM at temperatures of 27 °C in 5 mM sodium chloride solution. (D) Far-UV-circular dichorism spectra of 3.7 μM HSA measured in the absence (a) and presence of different concentrations of ButPd(II): 41.1 (b), 82.2 (c), and 123.2 (d) μM at temperature of 37 °C in 5 mM sodium chloride solution. (E) Far-UV-circular dichorism spectra of 3.7 μM HSA measured in the absence (a) and presence of different concentrations of EtPd(II): 41.1 (b), 82.1 (c), and123.2 (d) μM at temperatures of 27 °C in 5 mM sodium chloride solution. (F) Far-UV-circular dichorism spectra of 3.7 μM HSA measured in the absence (a) and presence of different concentrations of EtPd(II): 41.1 (b), 82.1 (c), and 123.2 (d) μM at temperatures of 37 °C in 5 mM sodium chloride solution.

that the binding constants (K) of ButPd(II) and OctPd(II) complexes are increased with the rising temperature from 27 to 37 °C, which indicated that the binding is endothermic ΔH (24.3 and 41.7 kJ/mol, respectively), and ΔS values are positive, which indicates that the binding processes are mainly entropy driven and that the enthalpy is unfavorable for them. Therefore, the thermodynamic parameters for the interaction of ButPd(II) and OctPd(II) and HSA can be explained on the basis of hydrophobic forces. However, in the case of the EtPd(II) complex, the binding reaction is exothermic (ΔH has small negative value) and like other complexes mainly entropy driven. Therefore, it might be concluded that hydrogen bonding addition of hydrophobic interaction might play a major role in the binding of the EtPd(II) complex to HSA.

ANS Fluorescence Studies. ANS is an extensively utilized fluorescent probe for the characterization of protein hydrophobic pockets. ANS binds in the hydrophobic subdomains (IIa and IIIa) of HSA. ANS fluorescence studies were carried out at two temperatures of 27 and 37 °C. In this study, first we incubated complexes and HSA for two minutes, and then ANS was added. After five minutes, emission of ANS was recorded and represented in Figure 6(A−F). Results of ANS fluorescence studies showed that interaction of the complexes and increase of temperature from 27 to 37 °C increase ANS fluorescence emission, meaning that complexes and temperature cause conformational changes that lead to the increase of nonpolar or hydrophobic surfaces of the protein to solvent environment. These results have a very good agreement with intrinsic fluorescence studies of the protein in the presence of different Pd(II) complexes that have shown 13−20 nm red shifts. Then, it can be concluded that these complexes induced relatively open structure in HSA.

CD Studies. CD has proven to be an ideal technique for monitoring conformational changes in proteins, which can occur as a result of changes in experimental parameters such as pH, temperature, and ligand binding, among others.[24] The far-UV-CD spectra characterize the secondary structure of proteins due to the peptide bond absorption, whereas the molar ellipticities at 222 nm ($[\theta]_{222}$) and 208 nm ($[\theta]_{208}$) or the ratio of $[\theta]_{208}/[\theta]_{222}$ have been typically used to characterize their α-helix content. The most abundant content of HSA is α-helix (almost about 60%), and there is no β-sheet content. The far-UV-CD spectrum of HSA in the absence and presence of different Pd(II) complexes with varying concentrations of 0, 100.4, 202.5, and 229.3 μM at two temperatures of 27 and 37 °C are shown in Figures 7(A−F) and Tables 2−4. From CD data, it can be concluded that the Pd(II) complexes can reduce the content of α-helix of protein accompanied by the increasing content of β-sheet structures of HSA. Then, these Pd(II) complexes can bind to HSA and induce a significant alteration in regular secondary structures of protein.[27,28]

DSC Studies. The study of HSA heat capacity against temperature in the presence of the Pd complexes was done by differential scanning calorimetry. As shown in Figure 8, the amount of heat capacity change for complexes increased. The transition points (T_m) of HSA in the absence and presence of different Pd(II) complexes were determined from transition point (T_m) and listed in Table 1. From these results, it can be concluded that different Pd(II) complexes significantly reduced the values of T_m and unstabilized the tertiary structure of HSA.

TABLE 2: Changes in Secondary Structure of HSA upon Interaction with the OcttPd(II) Complex at Different Temperatures

concentration (μM) at different temperatures (°C)	% α-helix	% β-sheet	% random coil
	27	59	5	36
0	37	61	5	34
	27	44	7	49
41	37	53	6	41
	27	43	7.5	49.5
82	37	44	7	49
	27	41	8	51
123	37	38	8	54

TABLE 3: Changes in Secondary Structure of HSA upon Interaction with the ButtPd(II) Complex at Different Temperatures

concentration (μM) at different temperatures (°C)	% α-helix	% β-sheet	% random coil
	27	60	4	36
0	37	61	4	35
	27	55	5	40
41	37	49	5	46
	27	46	7	46
82	37	43	7	50
	27	39	7.5	53.5
123	37	41	8	51

TABLE 4: Changes in Secondary Structure of HSA upon Interaction with the EtPd(II) Complex at Different Temperatures

concentration (μM) at different temperatures (°C)	% α-helix	% β-sheet	% random coil
	27	58	4	38
0	37	59	3	38
	27	50	5	45
41	37	49	5	46
	27	45	7	48
82	37	43	7	50
	27	42	7.5	50.5
123	37	42	8	50

The increase of changes of heat capacity show increasing hydrophobic surface area of the protein that has a good agreement with ANS studies.

Conclusion

Fluorescence intensity studies have shown that Pd(II) complexes have a strong ability to quench the intrinsic fluorescence of HSA. The number of binding sites and the association binding constant of Pd(II) complexes were calculated at 27 and 37 °C. The emission maximum shifted gradually to higher wavelength with the increase of drug concentrations, accompanying significant fluorescence quenching. It signified that the Trp and Tyr residues in protein have been brought to a more hydrophilic environment, and the conformation of protein has been changed due to the drug−HSA combination. Fluorescence studies showed that these Pd(II) complexes have great quenching property. Results of quenching showed that the Pd(II) complex with the ethylic hydrophobic chain has more powerful quenching property and in lower molar ratio thoroughly quenched HSA. Crystallography of HSA showed that the only tryptophan of HSA (TR 214) is located in the hydrophobic pocket in subdomain IIA and may be a Etpd(II) complex because it is a little smaller than the two other complexes, riche to fluorophore (Trp214) more quickly and easily than the other complexes do. The change in fluorescence intensity of Trp 214 in the presence of complexes may arise as a direct quenching or as a result of protein conformational changes induced by polymer−HSA complexation. The emission maximum of EtPd(II) and BuPd(II) complexes shifted gradually to higher wavelength with the increase of drug concentrations, accompanying significant fluorescence quenching, and the maximum red shift reached more than 12 and 20 nm, respectively. Also, the values of f_a increase by decreasing the size of the hydrophobic tail of the complexes that confirm quenching studies that revealed that complexes with longer hydrophobic tails have lower ability to quenching and accessibility to the Trp residue of the protein. The modified Stern−Volmer studies in two temperatures of 27 and 37 °C show that the fraction of fluorescence intensity accessible to the quencher increases by increasing temperature to 37 °C. ANS fluorescence and DSC studies in confirmation of each other reveal that interaction of complexes and increasing the temperature lead to transition of the inside hydrophobic part of HSA to the outside.

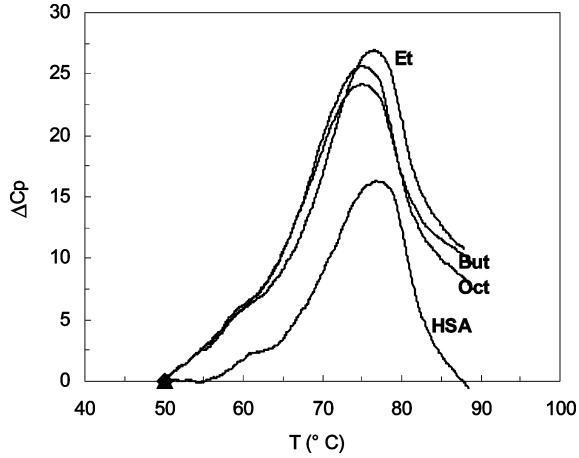

Figure 8. Plot of measured heat capacity against temperature for HSA in the absence and presence of different Pd(II) complexes.

From the above results, it can be concluded that binding of newly designed drugs (Pd(II) complexes) on the blood carrier protein of HSA resulted in significant changes on the structure and conformation of protein via decreasing stability of HSA by decreasing T_m, red shift in maximum fluorescence intensity, content of α-helical structure, and increasing nonpolar or accessible hydrophobic surface of protein to solvent.

Since the conformational changes in the carrier protein due to drug (the designed ligands) binding may have a deleterious effect, results obtained here from the interaction of the novel Pd(II) complexes with blood carrier protein, therefore, provide useful information to design better metal anticancer complexes with lower side effects in the future.

Abbreviations: HSA, human serum albumin; CD, circular dichroism; $\Delta H°$, enthalpy; $\Delta S°$, entropy; $\Delta G°$, Gibbs free energy; DSC, differential scanning calorimetry.

Acknowledgment. The financial support of the Research Council of the University of Tehran is highly appreciated.

References and Notes

(1) Wanga, T.; Xianga, B.; Wang, Y.; Chen, C.; Dong, Y.; Fang, H.; Wang, M. *Colloids. Surf. B: Biointerfaces* **2008**, *65*, 113.

(2) Meloun, B.; Morávek, L.; Kotska, V. *FEBS Lett.* **1975**, *58*, 134–137.

(3) Zunszain, P. A.; Ghuman, J.; Komatsu, T.; Tsuchida, E.; Curry, S. *BMC Struct. Biol.* **2003**, *3*, 6.

(4) Yamasaki, K.; Maruyama, T.; Kragh-Hansen, U.; Otagiri, M. *Biochim. Biophys. Acta* **1996**, *1295*, 147–157.

(5) Zhou, B.; Qi, Z. D.; Xiao, Q.; Dong, J. X.; Zhang, Y. Z.; Liu, Y. *J. Biochem. Biophys. Methods* **2007**, *70*, 743–747.
(6) Sulkowska, A. *J. Mol. Struct.* **2002**, *614*, 227–232.
(7) Yang, F.; Bian, C.; Zhu, L.; Zhao, G.; Huang, Z.; Huang, M. *J. Struct. Biol.* **2007**, *157*, 348–355.
(8) Ghuman1, J.; Zunszain1, P. A.; Ananyo, I. P.; Otagiri, M.; Curryl, S. *J. Mol. Biol.* **2005**, *353*, 38–52.
(9) Sułkowskaa, A.; Równicka, J.; Bojkoa, B.; Sułkowski, W. *J. Mol. Struct.* **2003**, 133–140.
(10) Petitpas, I.; Bhattacharya, A. A.; Twine, S.; East, M.; Curry, S. *J. Biol. Chem.* **2001**, *276*, 22804–22809.
(11) Budzisz, E.; Krajewska, U.; Rozalski, M. P. *J. Pharm.* **2004**, *56*, 473–478.
(12) Mansouri-Torshizi, H.; Srivastava, T. S.; Perekh, H. K.; Chitnis, M. P. *J. Inorg. Biochem.* **1992**, *45*, 135–148.
(13) Giovagnini, L.; Marzano, C.; Bettio, F.; Fregona, D. *J. Inorg. Biochem.* **2005**, *99*, 2139.
(14) Zhang, Q.; Zhong, W.; Xing, B.; Tang, W.; Chen, Y. *J. Inorg. Biochem.* **1998**, *72*, 195–200.
(15) Mansoori-Torshizi, H.; Islami-Moghaddam, M.; Saboury, A. A. *Acta Biochim. Biophys. Sin.* **2003**, *35*, 886–890.
(16) Wang, K.; Lu, J. F.; Li, R. C. *Coord. Chem. Rev.* **1996**, *151*, 53–88.
(17) Kasparkova, J.; Zehnulova, J.; Farrel, N.; Brabec, V. *J. Biol. Chem.* **2002**, *277*, 48076–48086.
(18) Divsalar, A.; Saboury, A. A.; Yousefi, R.; Moosavi-Movahedi, A. A.; Mansoori-Torshizi, H. *Int. J. Biol. Macromol.* **2006**, *40*, 381–386.
(19) Genova, P.; Varadinova, T.; Matsanz, A. I.; Marinova, D.; Souza, P. *Toxicol. Appl. Pharmacol.* **2004**, *197*, 107–112.
(20) Zhao, G.; Sun, H.; Lin, H.; Zhu, S.; Su, X.; Chen, Y. *J. Inorg. Biochem.* **1998**, *72*, 173–177.
(21) Mansouri-Torshizi, H.; I-Moghaddam, M.; Divsalar, A.; Sabory, A. A. *Bioorg. Med. Chem.* **2008**, *16*, 9616–9625.
(22) Yang, J. T.; Wu, C. S. C.; Martinez, H. M. *Anal. Chem.* **1981**, *53*, 778.
(23) Marthasarathy, P.; Johnson, W. C. J. *Anal. Biochem.* **1987**, *167*, 76.
(24) Hu, Y. J.; Liu, Y.; Pi, Z. B.; Qu, S. S. *Bioorg. Med. Chem.* **2005**, *13*, 6609–6614.
(25) Wang, Y. Q.; Zhang, H. M.; Zhang, G. C. *J. Pharm. Biomed. Anal.* **2006**, *41*, 1041–1046.
(26) Ambrosetti, R.; Bianchini, R.; Fischella, S.; Fichera, M.; Zandomeneghi, M. *Chem.—Eur. J.* **1996**, *2*, 149–156.
(27) He, X. M.; Carter, D. C. *Nature* **1992**, *358*, 209–215.
(28) Lakowicz, J. R. *Principles of Fluorescence Spectroscopy*, 2nd ed.; Kluwer Academic Publishers/Plenum Press: New York, 1999.
(29) Ghuman, J.; Zunszain, P. A.; Petitpas, I.; Bhattacharya, A. A.; Otagiri, M.; Curry, S. *J. Mol. Biol.* **2005**, *353*, 38–52.
(30) Qi, Z. D.; Zhou, B.; Xiao, Q.; Shi, C.; Liu, Y.; Dai, J. J. *Photochem. Photobiol. A: Chem.* **2008**, *193*, 81–88.
(31) Maiti, T. K.; Ghosh, K. S.; Samanta, A.; Dasgupta, S. J. *Photochem. Photobiol. A: Chem.* **2008**, *194*, 297–307.
(32) Li, J.; Ren, C.; Zhang, Y.; Liu, X.; Yao, X.; Hu, Z. *J. Mol. Struct.* **2008**, *885*, 64–69.
(33) Zhang, Y.; Que, Q.; Pan, J.; Guo, J. *J. Mol. Struct.* **2008**, *881*, 132–138.
(34) Sułkowska, A. *J. Mol. Struct.* **2002**, *614*, 227–232.
(35) Sulkowska, A.; Rownicka, J.; Sułkowski, W. *J. Mol. Struct.* **2003**, *651−653*, 133–140.
(36) Froehlich, E.; Mandeville, J. S.; Jennings, C. J.; Sedaghat-Herati, R.; Tajmir-Riahi, H. A. *J. Phys. Chem. B* **2009**, *113*, 6986.
(37) Barik, A.; Mishra, B.; Kunwar, A. *Chem. Phys. Lett.* **2007**, *436*, 239–243.
(38) Hu, Y. J.; Liu, Y.; Zhao, R. M.; Qu, S. S. *Int. J. Biol. Macromol.* **2005**, *37*, 122–126.

JP904822N